

## ORIGINAL ARTICLE

# Genotype–phenotype correlation in patients with isovaleric acidaemia: comparative structural modelling and computational analysis of novel variants

Osama K. Zaki<sup>1</sup>, George Priya Doss C<sup>2</sup>, Salsabil A. Ali<sup>3</sup>, Ghadeer G. Murad<sup>3</sup>, Shaima A. Elashi<sup>3</sup>, Maryam S.A. Ebnou<sup>3</sup>, Thirumal Kumar D<sup>2</sup>, Ola Khalifa<sup>1</sup>, Radwa Gamal<sup>1</sup>, Heba S.A. El Abd<sup>1</sup>, Bilal N. Nasr<sup>3</sup> and Hatem Zayed<sup>3,\*</sup>

<sup>1</sup>Department of Medical Genetics, Ain Shams Paediatrics Hospital, Cairo, Egypt, <sup>2</sup>Department of Integrative Biology, School of Biosciences and Technology, VIT University, Vellore 632014, Tamil Nadu, India and

<sup>3</sup>Department of Biomedical Sciences, College of Health Sciences, Qatar University, Doha, Qatar

\*To whom correspondence should be addressed at: Department of Biomedical Sciences, College of Health Sciences, Qatar University, P.O.Box: 2713, Doha, Qatar. Tel: +974 44034809; Fax: +974 44031351; Email: hatem.zayed@qu.edu.qa

## Abstract

Isovaleric acidaemia (IVA) is an autosomal recessive inborn error of leucine metabolism. It is caused by a deficiency in the mitochondrial isovaleryl-CoA dehydrogenase (IVD) enzyme. In this study, we investigated eight patients with IVA. The patients' diagnoses were confirmed by urinary organic acid analysis and the blood C5-Carnitine value. A molecular genetic analysis of the IVD gene revealed nine different variants: five were missense variants (c.1193G > A; p. R398Q, c.1207T > A; p. Y403N, c.872C > T; p. A291V, c.749G > C; p. G250A, c.1136T > C; p.I379T), one was a frameshift variant (c.ins386 T; p. Y129fs), one was a splicing variant (c.465 + 2T > C), one was a polymorphism (c.732C > T; p. D244D), and one was an intronic benign variant (c.287 + 14T > C). Interestingly, all variants were in homozygous form, and four variants were novel (p. Y403N, p. Y129fs, p. A291V, p. G250A) and absent from 200 normal chromosomes. We performed protein modelling and dynamics analyses, pathogenicity and stability analyses, and a physicochemical properties analysis of the five missense variants (p.Y403N, R398Q, p.A291V, p.G250A, and p.I379T). Variants p.I379T and p.R398Q were found to be the most deleterious and destabilizing compared to variants p.A291V and p.Y403N. However, the four variants were predicted to be severe by the protein dynamic and *in silico* analysis, which was consistent with the patients' clinical phenotypes. The p.G250A variant was computationally predicted as mild, which was consistent with the severity of the clinical phenotype. This study reveals a potentially meaningful genotype-phenotype correlation for our patient cohort and highlights the development and use of this computational analysis for future assessments of genetic variants in the clinic.

## Introduction

Isovaleric acidaemia (IVA; MIM #243500) is an autosomal recessive inborn error of leucine metabolism caused by a deficiency in the isovaleryl-CoA dehydrogenase (IVD; NM\_002225.3 and NP\_002216.2) (1). The precursor for the IVD protein consists of

426 amino acid residues, while the mature protein consists of 394 amino acid residues (2). Clinically, patients with IVA are characterized by vomiting, poor feeding, lack of energy, and an odour of "sweaty feet". Biochemically, they are characterized by an accumulation of isovaleric acid, 3-hydroxyisovaleric acid, isovaleryl-carnitine (C5), and isovaleryl glycine (IVG) in cells,

Received: April 28, 2017. Revised: April 18, 2017. Accepted: May 16, 2017

© The Author 2017. Published by Oxford University Press. All rights reserved. For Permissions, please email: journals.permissions@oup.com

blood, and urine, which is associated with ketoacidosis and hyperammonaemia (3). Clinical variations, ranging from acute neonatal to chronic intermittent, are frequently observed among patients with IVA (4–7), even among genetically homogeneous populations (8).

The IVD gene is located on 15q14-15 and consists of 12 exons spanning 15 kb. According to the Human Gene Mutations Database (HGMD) ([www.hgmd.org](http://www.hgmd.org)), over 67 variants have been reported in the human IVD gene. The genotype–phenotype correlation in the IVA due to these variants is not straightforward, and a meaningful correlation remains questionable, in part due to the variability of the clinical presentation and heterogeneity of the disease. However, some variants are known to be causative for the disease and frequent among certain ethnic groups, such as the p.A314V variant (originally reported as p.A282V, based on the mature protein) in Caucasians (4) and the p.G123R variant in Caucasians of South Africa (8). Among the East and Southeast Asian populations, the variants p.Y403C (originally reported as p.Y403C) and c.466-3\_2CA > GG (originally reported as c.457-3\_2CA > GG, according to NM\_002225.2 (previous version)) were frequently observed in Taiwan (9), Korea (10), and Thailand (7). In this study, we investigated the clinical, biochemical, and molecular genetic profiles of eight Egyptian patients who were diagnosed with IVA. We identified nine different variants in the IVD gene in these patients who were comprehensively analysed using an intensive computational analysis.

## Materials and Methods

### MS/MS

Blood samples were obtained through finger pricks of the eight patients and placed on a Guthrie card (Whatman 903 filter paper, GE Healthcare, New Jersey, USA). The blood spots were analysed for an amino acids/acyl-L-carnitine profile using a triple, quadruple tandem mass spectrometer (ACQUITY UPLC H-Class, Waters® Corporation, Massachusetts, USA), with a positive electrospray ionization probe utilizing the Mass Chrom® amino acids and acyl-carnitine Dried Blood kit (Chromsystems Instruments and Chemicals GmbH, München, Germany) per the manufacturer's instructions. The data from the Multiple Reaction Monitoring (MRM) scan were analysed using the Masslynx and Neolynx® applications (Waters® Corporation, Massachusetts, USA).

### GC/MS

The urine from each patient was collected and frozen until derivatization by silylation of organic compounds. The MS/MS analysis was performed using the Agilent 7890 system gas chromatography instrument interfaced with a Model 5975 mass spectrometer and a gas chromatography capillary column HP 5MS (25 × 0.2 mm i.d., 0.33 µm film, Agilent, USA). The column temperature was initially maintained at 80 °C for 2 min and then increased from 80 °C to 280 °C by 4 °C/min, where it was held for 3 min. The run time was 55 min. The organic acid profile was visually compared with normal control samples and the standard organic acids of interest.

### Molecular genetic analysis

After written consent was obtained from each patient's family, the genomic DNA samples of the eight patients were collected,

and the 12 exons, exon-intron junctions, and promoter regions of the IVA gene (NM\_002225.3) were sequenced using the GENEWIZ, Inc. sequencing service (South Plainfield, NJ) using Applied Biosystems BigDye version 3.1. The reactions were run on the Applied Biosystems 3730XL DNA Analyser. Both the forward and reverse strands were sequenced. The sequencing data were analysed using the Lasergene SeqMan software (DNASTAR, Madison, WI) to detect any mutations compared to the genomic DNA reference sequence.

### Dataset

The FASTA sequence and native structure of the IVD were retrieved from the NCBI (NP\_002216.2) and Protein Data Bank (PDBID: 1IVH) databases, respectively. The crystallized protein structure consists of 394 amino acids (30–423) with a resolution of 2.60 Å. Residues and their corresponding positions for variants p.Y403N, p.Y129fs, p.A291V, p.G250A, and p.I379T were identified and submitted as the input to an *in silico* tool prediction and structural analysis.

### Pathogenicity and stability analysis

The pathogenicity and stability changes upon mutation were predicted using the PredictSNP (11) and iStable servers (12). In addition to its own prediction, PredictSNP contains the results from other pathogenic predictors such as MAPP, PhD-SNP, PolyPhen-1, PolyPhen-2, SIFT, SNAP, nsSNP Analyzer and PANTHER. Similarly, the protein stability predictor iStable predicts stability through its own algorithm and provides the results from other stability predictors such as I-mutant2 and MUpro. The impact of variation at the intron was analysed using the Human Splicing Finder (13). The FASTA sequence obtained from the NCBI and SNP information was provided as the input for the analysis.

### Physicochemical property analysis

The change in the properties of the native amino acids due to the mutation might induce higher pathogenicity and destabilize the protein (14,15). The changes in the properties of the native and variant amino acids were predicted using NCBI Amino Acid Explorer. Seven parameters including the change in hydrophobicity, charge, polarity, side chain flexibility, interaction mode, aliphatic/aromatic nature and R' group were considered for our analysis.

### Protein modelling and macromolecule dynamics

The native molecule was individually mutated and energy-minimized from glycine to alanine, alanine to valine, isoleucine to threonine, arginine to glutamine and tyrosine to asparagine at their corresponding positions: 250, 291, 379, 398, and 403, respectively, using the SwissPDB viewer (16). Furthermore, the native and mutated molecules were subjected to a Macromolecule dynamics study using GROMACS v4.5.6 (17) to understand the structural changes in the protein upon mutation. The GROMACS supporting files were generated using pdb2gmx. Simple Point Charge was used to solvate the molecule in a cubical box within 10 Å. The system was neutralized using counter ions. The neutralized system was equilibrated using NVT and NPT ensembles for each 500 ps. Finally, the system was subjected to molecular dynamics simulation for 30 ns, and

trajectories were obtained as the output. The trajectories were analysed using *g\_rmsd*, *g\_rmsf*, *g\_hbond* and *g\_gyrate* to study the root mean square deviation (RMSD), root mean square fluctuation (RMSF), intramolecular hydrogen bonds (Hbonds) and RoG, and graphs were plotted using Grapher. The secondary structure of the protein was visualized using the DSSP plugin of PyMOL.

## Patient data

A total of eight Egyptian patients from unrelated families with IVA were recruited at the Metabolic Clinic, Ain Shams University, Cairo, Egypt. All patients were diagnosed based on their clinical presentation and IVA-specific metabolites in the plasma and urine and confirmed by molecular genetic testing. Informed consent was obtained from each patient's family, and the study was approved by the ethics committees of the University of Ain-Shams, Faculty of medicine and in compliance with the 1964 Helsinki Declaration and its recent amendments. The available clinical, biochemical, and organic acid profiles are summarized in Table 1 for all patients. To compare the degree of morbidity between the individual families, we classified the examined families into acute neonatal or chronic intermittent types according to age and mode of disease onset, presenting symptoms, age at diagnosis, neurological sequelae and the clinical history of other affected siblings.

## Results

### Molecular genetic analysis

All 12 exons, exon-intron junctions (at least 50 nt), and promoter regions (at least 150 nt) in the IVD gene were screened by Sanger sequencing in the eight Egyptian patients who were diagnosed with IVA. Nine variants were identified: five were missense variants (c.1193G > A; p. R398Q, c.1207T > A; p. Y403N, c.872C > T; p. A291V, c.749G > C; p. G250A, c.1136T > C; p. I379T), one was a frameshift (c.ins386 T; p. Y129fs), one was a splicing variant (c.465 + 2T > C), one was a polymorphism (c. 732C > T; p. D244D), and one was an intronic benign variant, c.287 + 14T > C, which was reported in the dbSNP with rs2289331 (Fig. 1 and Table 2). Interestingly, all variants were homozygous.

The c.243 + 14T > C variant was found in all patients. The p.R398Q variant was previously reported in an Omani patient with IVA (18). The previously reported variant c.465 + 2T > C (19) was detected in patient #6. Four variants, p.Y403N, p.Y129fs, p.A291V, and p.G250A, were found to be novel (Table 2) and were not found in dbSNP (<http://www.ncbi.nlm.nih.gov/projects/SNP/>), the Human Genetic Variation Browser (<http://www.hgvd.genome.med.kyoto-u.ac.jp/>), the Exome Variant Server (<http://evs.gs.washington.edu/EVS/>), HGMD, or any reported cases to date. In addition, these novel variants were absent from 100 normal individuals (200 normal chromosomes) of mostly Arab descent.

### Clinical and biochemical diagnosis of IVA patients

All patients were products of consanguineous marriages, the male:female ratio was 5:3, the current age of the patients ranged from 1.5 to 8 years, the age at diagnosis ranged from the time of birth to 72 months, and the age of onset ranged from 3 days to 12 months (Table 1).

Patient #1 is a four-year-old boy, Twin A, and the 4<sup>th</sup> child of a consanguineous marriage. He was diagnosed at the age of 3

Table 1. Clinical and biochemical analyses of patients with IVA

P#	Age (y)	AO/AD	Sex	CS	Clinical presentations	Type	Diet	Urine Organic acids	C5-carnitine (0.0–0.52 μmol/l)
1	4	–/3 d	M	+	NA	acute neonatal	IVA special formula	Elevated isovalerylglycine	6.15
2	4	4 m/13 m	F	+	Cyclic vomiting, coma	chronic intermittent	Vegetarian	Abnormal excretion of isovalerate metabolites-lactic aciduria	16
3	4.5	–/birth	F	+	NA	acute neonatal	–IVA special formula-Vegetarian diet	Elevated isovalerylglycine	10.8
4	2.5	5 d/30 d	M	+	Poor suckling, lethargy, hyperammonaemia and thrombocytopenia	acute neonatal	–IVA special formula	Elevated isovalerylglycine	17.4
5	7	12 m/60 m	M	+	Cyclic vomiting requiring admission every three months	chronic intermittent	–Vegetarian diet	Elevated isovalerylglycine	4.6
6	8	6 m/72 m	M	+	Three Monthly attacks of cyclic vomiting	chronic intermittent	IVA special formula	Elevated isovalerylglycine	9.06
7	1.9	3 d/10 d	F	+	Lethargy, poor feeding, Convulsions, encephalopathy	acute neonatal	IVA special formula	Elevated isovalerylglycine	2.45
8	6	–/3 d	M	+	NA	acute neonatal	IVA special formula	Elevated isovalerylglycine	6.8

P#, patient number; y, year; CS, consanguinity; M, male; F, female; AO, Age of onset; AD, Age of diagnosis; NA, not available.

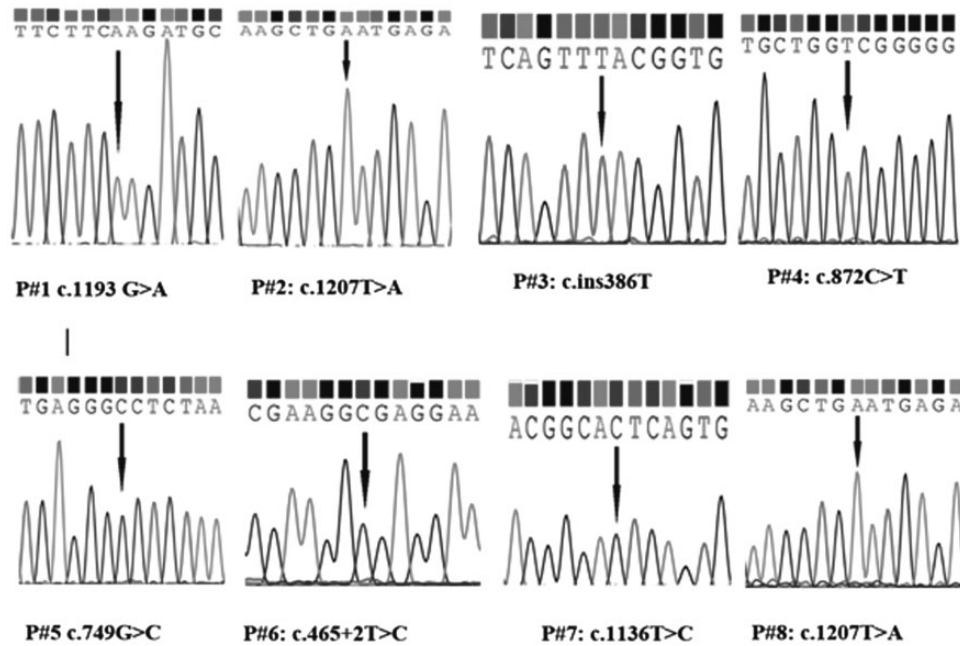


**Figure 1.** The Sanger sequencing results for the eight pathogenic mutations. All mutations are in homozygous form. The polymorphism c.732C>T; p. D244D and the recurrent benign allele c.287 + 14T>C (rs2289331) are not shown. \*c.287 + 14T>C was observed in all patients.

**Table 2.** Molecular genetic analysis of patients with the IVD variants

P #	Nt change	Allele frequency	AA change	Exon/ Intron	References
1	c.1193G>A	2/16	p.R398Q	Exon12	(18)
	c.287 + 14T>C*	2/16	NA	Intron2	dbSNP
2	c.1207T>A	2/16	p.Y403N	12	This Study
	c.287 + 14T>C*	2/16	NA	Intron 2	dbSNP
3	c.ins386 T	2/16	p.Y129fs	4	This Study
	c.732C>T	2/16	p.D244D	7	dbSNP
4	c.287 + 14T>C*	2/16	NA	Intron 2	dbSNP
	c.872C>T	2/16	p.A291V	8	This Study
5	c.287 + 14T>C*	2/16	NA	Intron 2	dbSNP
	c.749G>C	2/16	p.G250A	7	This Study
6	c.287 + 14T>C*	2/16	NA	Intron 2	dbSNP
	c.465 + 2T>C	2/16	NA	Intron 4	(19)
7	c.287 + 14T>C*	2/16	NA	Intron 2	dbSNP
	c.1136T>C	2/16	p.I379T	11	(1)
8	c.287 + 14T>C*	2/16	NA	Intron 2	dbSNP
	c.1207T>A	2/16	p.Y403N	12	This Study
	c.287 + 14T>C*	2/16	NA	Intron 2	dbSNP

P#, patient number; Nt, nucleotide; AA, amino acid. The reference number used: NM\_002225.3; NP\_002216.2.

days during newborn screening due to a positive family history of three sibling deaths (Fig. 2A). At the age of 3 days, he showed elevated C5-carnitine at 6.5  $\mu\text{mol/l}$  (reference range 0.0–0.52  $\mu\text{mol/l}$ ), and the diagnosis of IVA was confirmed by elevated isovaleryl glycine in the urine organic acid profile. He started on a special milk formula, and by 2 years of age, he stopped the formula and remained on a vegetarian diet with L-carnitine. Since then, he has been admitted every 3 to 4 months with a metabolic crisis. At the age of 4 years, he started again on the special milk formula, together with the vegetarian diet with L-carnitine. The last hospital admission was 2 months ago with an acute metabolic crisis. The patient started to sit alone at 6 months,

walked alone at 1 year, and spoke his first word at one year. An unremarkable systemic examination was noted during his physical examination at 4 years of age.

Patient #2 is a 5.5-year-old female, the 4<sup>th</sup> in the order of birth of consanguineous parents. She was a full-term delivery by Caesarean section (CS) due to a failure of propagation. Her body weight was 2 kg. She appeared normal and was discharged on the 2<sup>nd</sup> day. At the age of 2 months, she experienced cyclic vomiting every three weeks. At the age of 1.1 years, she developed vomiting and coma and was admitted to the ICU for 10 days where she was diagnosed by extended metabolic screening as a case of IVA with C5-carnitine at 16  $\mu\text{mol/l}$  and marked elevation of isovaleryl glycine in the urine. She began a vegetarian diet plus L-carnitine. At 2 years, she was admitted for 10 days because of vomiting and acidosis. No further hospital admissions have since been reported. On physical examination at 5.5 years of age, her weight was 18 kg (5<sup>th</sup> percentile) and height was 103 cm (33<sup>rd</sup> percentile); she had an unremarkable systemic examination and her intellectual quotient (IQ) was 92.

Patient #3 is a 4.5-year-old female, the 3<sup>rd</sup> of a consanguineous marriage, who has been admitted to the NICU since birth due to a previous history of sibling deaths (Fig. 2B). She was referred to our genetic unit for the stat MS/MS newborn screening, and the diagnosis of IVA was established the next day; MS/MS showed C5-carnitine at 10.8  $\mu\text{mol/l}$  (reference range 0.0–0.52  $\mu\text{mol/l}$ ), and the urinary organic acid analysis showed moderate to marked elevations in lactic acid, 3-hydroxy-isovaleric acid and isovaleryl glycine and minimal elevation of 3-hydroxy butyric and acetoacetic acid. She started the IVA dietary regimen in the form of a special formula together with oral glycine and oral L-carnitine. She had fluctuating levels of serum ammonia, and oral sodium benzoate was initially started and then discontinued at the age of 3 months after successive monitoring with normal serum ammonia levels. She stopped formula intake at 2 years of age but continued the vegetarian diet. She had only two hospital admissions throughout her 4.5-year lifetime. The first admission at the age of 4 years was due to a presentation of gastroenteritis with

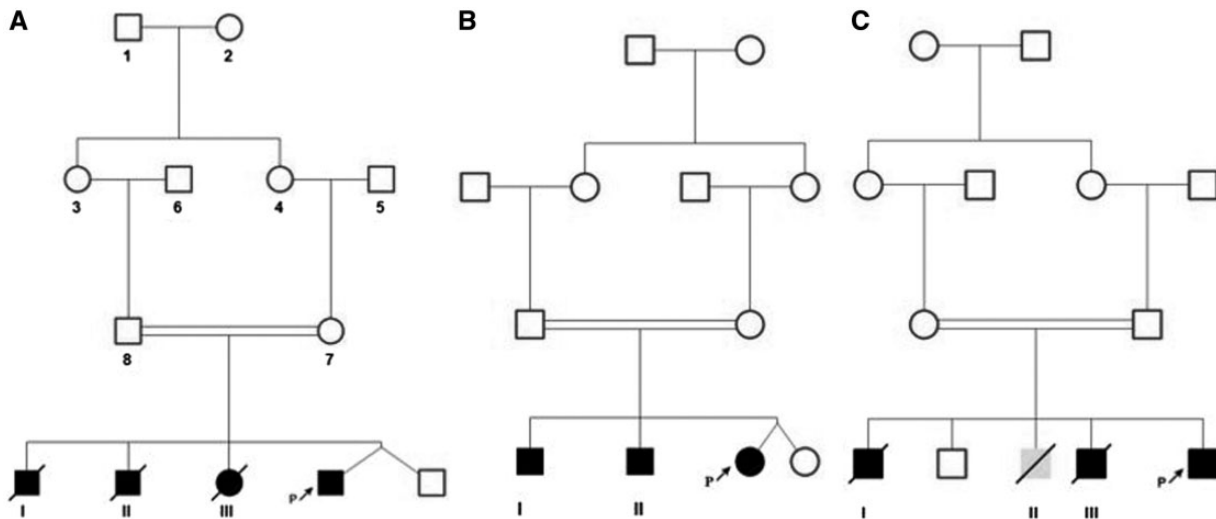


**Figure 2.** (A) I: he was admitted to the NICU on the second day for jaundice, poor suckling, lethargy, and coma for 1 week and died at the age of 10 days. II: he was well until 7 days. He then showed poor suckling, lethargy, coma and was admitted to the NICU and died at the age of 11 days. III: she was diagnosed as IVA after coma at the age of 10 days. She started a special formula with subsequent improvement and a shift to low protein intake. Later, she abandoned the dietary regimen & was admitted at 3.5 years of age with gastroenteritis and acidosis, placed on ventilator and died. (B) I: he was normal until 3 days; then, he developed poor suckling and lethargy, was admitted to the NICU, placed on a ventilator and died at the age of 15 days. II: he was normal until 3 days, and then, lethargy, poor suckling, hyperammonaemia developed; He was placed on a ventilator and died at the age of 21 days. (C) I: he was normal until 1 week. Then, he had poor suckling, lethargy, coma and was admitted to the NICU and died at the age of 20 days. II: he had hydrocephalus and meningocele, was admitted at 2 months for a shunt operation and died of complications at 5 months. III: he was normal until 1 week. Then, poor suckling and coma occurred, and the patient was admitted to the NICU with hyperammonaemia (500  $\mu\text{Mol/l}$ ), and death occurred at the age of 1 month.

metabolic acidosis necessitating intravenous fluids and intravenous sodium bicarbonate. The second admission at the age of 4.5 years was due to persistent vomiting with a diagnosis of acute pancreatitis. She had acidosis that required oral intake of sodium bicarbonate for two months after discharge. She could sit unsupported at 6 months, walked at 12 months, and spoke her first word at 12 months. On physical examination at 4.5 years, her height was 105 cm (55<sup>th</sup> percentile), weight was 18 kg (67<sup>th</sup> percentile); her neurologic, chest, cardiovascular, and abdominal examinations were unremarkable.

Patient #4 is a 2.5-year-old boy, the fourth of a consanguineous marriage. His body weight was 3 kg, and apart from a history of one month of maternal bleeding due to placenta previa, the pregnancy was uneventful. On the 2<sup>nd</sup> day after delivery, he began to refuse breast-feeding. On the 4<sup>th</sup> day, he experienced vomiting, and on the 5<sup>th</sup> day, he became lethargic. He was admitted to the NICU as a case of suspected sepsis receiving intravenous fluids and a one-time platelet transfusion for thrombocytopenia. On the 10<sup>th</sup> day, his blood ammonia level was 500  $\mu\text{mol/l}$ . At the age of one month, he was referred to our genetics unit for a consultation where the diagnosis of IVA was established. His MS/MS showed C5-carnitine at 17.4  $\mu\text{mol/l}$  (0.0–0.52  $\mu\text{mol/l}$ ). The urinary organic acid analysis showed marked elevations of isovaleryl glycine. He started on special IVA formula, sodium benzoate, and glycine. After a sustained normal ammonia level for one month of treatment, sodium benzoate was discontinued. The patient also discontinued oral glycine after one year. There is no history of hospital admission since birth. He started to sit at 6 months, walked at 13 months, and started to babble at 17 months of age, with no bladder or bowel control until the age of 2.5 years; his weight was 14 kg (11<sup>th</sup> percentile) and height was 86.5 cm (65<sup>th</sup> percentile). No other systemic abnormalities were noted.

Patient #5 is a seven-year-old boy, and his body weight was 3.5 kg. He had a history of an elder sister who exhibited poor

suckling since birth and died at the age of 7 days. He was admitted at the age of 7 days to the NICU due to vomiting and a refusal to feed. However, he was discharged one day later. The severe symptoms started at the age of 1 year. The patient had repeated attacks of lethargy, an abnormal odour of urine, and vomiting without fever or diarrhoea. He was admitted to the hospital for 1 week, administered antiemetic drugs, and discharged. At the age of 1.3 years, he had vomiting that was not associated with fever or diarrhoea, was admitted to the hospital for 2 days and was restarted on antiemetics and IV fluids. He had repeated attacks of vomiting every 1–2 months and frequent hospital admissions that lasted several days, where he was administered IV fluids and discharged. At the age of five years, he was admitted to our hospital for 10 days for vomiting as a case that was diagnosed with IVA. His MS/MS showed elevated C5-carnitine at 4.5  $\mu\text{mol/l}$  (0.0–0.52  $\mu\text{mol/l}$ ). The urinary organic acid analysis showed marked elevations of isovaleryl glycine. He started a vegetarian diet with L-carnitine, and the vomiting subsequently stopped. At 5 years and 2 months, and against the physician's advice, he consumed a protein meal with meat and chicken. As a result, he became lethargic and started vomiting due to severe metabolic acidosis. When he was 7 years of age, he again consumed the same diet, and he suffered from metabolic acidosis and persistent vomiting. He had abnormal electrocardiogram (EKG), and an echocardiogram (ECHO) was recommended. The ECHO revealed a dilated aortic root and a mild aortic regurgitation for follow-up. He started to sit at 6 months, walked at 1.2 years, and spoke his first word at 1 year. On physical examination, his height was 128 cm (88<sup>th</sup> percentile), his weight was 18 kg (11<sup>th</sup> percentile) and no other abnormalities were noted.

Patient #6 is an eight-year-old boy. He is the second in the order of birth of a consanguineous marriage. He began vomiting at the age of 6 months without fever or diarrhoea and took antiemetic drugs with a mild improvement. At the age of

**Table 3.** Pathogenicity and Stability of the missense variants in patients #1, 2, 4, 5, 7, and 8

Mutation	p.G250A	p.A291V	p.I379T	p.R398Q	p.Y403N
I-mutant2	<b>Decrease</b>	Increase	<b>Decrease</b>	<b>Decrease</b>	<b>Decrease</b>
MUpro	<b>Decrease</b>	Increase	<b>Decrease</b>	<b>Decrease</b>	<b>Decrease</b>
iStable	<b>Decrease</b>	Increase	<b>Decrease</b>	<b>Decrease</b>	<b>Decrease</b>
PredictSNP	Neutral	<b>Pathogenic</b>	<b>Pathogenic</b>	<b>Pathogenic</b>	Neutral
MAPP	Neutral	<b>Pathogenic</b>	<b>Pathogenic</b>	Neutral	Neutral
PhD-SNP	Neutral	<b>Pathogenic</b>	<b>Pathogenic</b>	<b>Pathogenic</b>	<b>Pathogenic</b>
PolyPhen-1	Neutral	<b>Pathogenic</b>	<b>Pathogenic</b>	<b>Pathogenic</b>	Neutral
PolyPhen-2	<b>Pathogenic</b>	<b>Pathogenic</b>	<b>Pathogenic</b>	<b>Pathogenic</b>	<b>Pathogenic</b>
SIFT	<b>Pathogenic</b>	<b>Pathogenic</b>	<b>Pathogenic</b>	<b>Pathogenic</b>	<b>Pathogenic</b>
SNAP	Neutral	<b>Pathogenic</b>	Neutral	<b>Pathogenic</b>	Neutral
nsSNP Analyzer	<b>Pathogenic</b>	Neutral	Neutral	Neutral	<b>Pathogenic</b>
PANTHER	Neutral	<b>Pathogenic</b>	<b>Pathogenic</b>	<b>Pathogenic</b>	Neutral

Variants that are deleterious and destabilizing to the protein are highlighted in bold.

9 months, he was admitted to the hospital for 2 days for vomiting. He had attacks of vomiting every three months. When he was 6 years old, he was diagnosed by extended metabolic screening based on elevated C5-carnitine at 9.06  $\mu\text{mol/l}$ , with a marked elevation in isovaleryl glycine in the urine. The condition resolved after the intake of a vegetarian diet with L-carnitine. At the age of 7 years, he was admitted to the hospital for asthmatic bronchitis and discharged on bronchodilators. He sat at 9 months, walked at 15 months and spoke one word at 17 months. At the age of 8 years, his height was 133.5 cm (84<sup>th</sup> percentile) and weight was 29 kg (74<sup>th</sup> percentile). Otherwise, he had an unremarkable systemic examination.

Patient #7 is a 1.9-year-old female. She became lethargic with poor feeding that progressed to coma and was admitted to the NICU at the age of 4 days. She was sleepy and refused feedings. On day 9, her conditions worsened with a poor response to painful stimuli that progressed to coma on the same day. She was investigated for the possibility of IEM and diagnosed with IVA 1 day later based on an elevated level of C5-carnitine, 2.45  $\mu\text{mol/l}$ , and elevated isovaleryl glycine in her urine GC/MS profile. Her dietary treatment started in the form of a special milk formula, L-carnitine, and supplementary glycine. Eight days later, she regained consciousness and was discharged at 17 days old. She continued the glycine intake for 8 months, and she remained on a leucine-restricted diet with L-Carnitine. The patient is now on 1 gm/kg natural protein with 0.5 gm/kg protein from the leucine-free formula. Her weight was 11 kg (54<sup>th</sup> percentile) and height was 90 cm (94<sup>th</sup> percentile). She is now achieving normal milestones with a normal neurological examination.

Patient #8 is a six-year-old boy and the 5<sup>th</sup> in the order of birth of a consanguineous marriage. He was diagnosed on the 3<sup>rd</sup> day of life during newborn screening due to a positive family history of multiple sibling deaths (Fig. 2C). He showed elevated C5-Carnitine at 6.8  $\mu\text{mol/l}$  at the time of diagnosis with a marked elevation of isovaleryl glycine. He started the IVA formula and oral L-carnitine. S. ammonia was high on the second day and became normal after starting the treatment. A squint was noticed at the age of 6 months. At the age of 4 years, he had an operation for the squint after a failure to correct the diplopia with glasses. The patient showed normal development for his age. On a physical examination at 6 years of age, his height was 128 cm (98<sup>th</sup> percentile) and weight was 28 kg (98<sup>th</sup> percentile). He had a normal chest, cardiovascular and abdominal examination.

### Pathogenicity and stability analysis

Twelve different *in silico* tools were used for predicting the pathogenicity and stability of the five missense variants p.G250A, p.A291V, p.I379T, p.R398Q, and p.Y403N. Ten tools predicted the variants p.I379T and p.R398Q to be pathogenic and destabilizing to the IVD protein, followed by variant p.A291V, which was predicted as pathogenic and destabilizing by 8 tools. Finally, the variants p.Y403N and p.G250A were predicted as pathogenic and destabilizing by 7 and 6 tools, respectively (Table 3).

### Physiochemical property analysis

The physiochemical properties of the amino acids were analysed using NCBI Amino Acid Explorer. We evaluated our mutants using seven physiochemical parameters (Table 4). The variant p.I379T exhibited changes in five physiochemical properties (hydrophobic to hydrophilic, non-polar to polar, moderate side chain flexibility to low chain flexibility and an R' group change from methylene to hydroxyl). The second most physiochemically affected variant was the variant p.R398Q, which exhibited changes in three physiochemical properties (hydrophobic to hydrophilic, positive to neutral and an R' group change from methylene to amide). The variant p.Y403N exhibited changes in two physiochemical properties (hydrophobic to hydrophilic and an R' group change from hydroxyl to amide), and the variants p.A291V and p.G250A, which were predicted as pathogenic and destabilizing by eight and six tools, respectively, exhibited changes in side chain flexibility alone (limited to low and limited to none) (Table 4A–E).

### Macromolecule dynamics

Macromolecule dynamics was performed using the GROMACS v.4.5.6 package for 30 ns for all five missense variants. Root mean square deviation (RMSD) was analysed, and the graph was plotted to study the convergence of the protein over a period of 30 ns. The overall deviation patterns of the proteins were between ~0.2 nm and ~0.4 nm. Initially, a larger deviation pattern was observed in the trajectory files that might have been due to the kinetic shock introduced during the initial phase of the molecular dynamics simulation. Finally, at the end of 30 ns, all the molecules were found to be stable and converged. Although a comparable deviation pattern was observed in the RMSD plot for all the variants and native proteins, the variants p.I379T and p.R398Q showed relatively higher deviating

Table 4. Change in the physicochemical properties of the native and mutant amino acids using the NCBI Amino Acid Explorer prediction tool

Physicochemical properties	p.G250A		p.A291V		p.I379T		p.R398Q		p.Y403N	
	Glycine	Alanine	Alanine	Valine	Isoleucine	Threonine	Arginine	Glutamine	Tyrosine	Asparagine
Native & variant amino acids										
<b>Hydrophobicity</b>	Hydrophobic	hydrophobic	hydrophobic	hydrophobic	hydrophobic	hydrophilic	hydrophilic	hydrophilic	hydrophobic	hydrophilic
<b>Charge</b>	Neutral	Neutral	Neutral	Neutral	Neutral	Neutral	Positive	Neutral	Neutral	Neutral
<b>Polarity</b>	Non-polar	Non-polar	Non-polar	Non-polar	Non-polar	Polar	Polar	Polar	Polar	Polar
<b>Side chain flexibility</b>	Limited	Limited	Limited	Low	Moderate	Low	High	High	Moderate	Moderate
<b>Interaction modes</b>	van der Waals	H-bonds, van der Waals	Ionic, H-bonds, van der Waals	Ionic, H-bonds, van der Waals	H-bonds, aromatic stacking, van der Waals	H-bonds, van der Waals				
<b>Aliphatic/Aromatic R Group</b>	Aliphatic	Aliphatic	Aliphatic	Aliphatic	Aliphatic	Aliphatic	Aliphatic	Aliphatic	Aromatic	Aromatic
	Methylene	Methylene	Methylene	Methylene	Methylene	Hydroxyl	Methylene	Amide	Hydroxyl	Amide

patterns compared to the other three missense variants and native proteins (Fig. 3A). The stable converged system was further analysed for root mean square fluctuation (RMSF), Hbonds and RoG.

The RMSF analysis was utilized to further demonstrate the importance of each amino acid residue and their participation in structural fluctuation. A variable fluctuation pattern was observed in all variant proteins when compared to the native protein. A high level of residual fluctuation was observed in the variant p.I379T (Fig. 3B). The RoG was performed to evaluate the compactness levels of the variants versus the native protein, and the variant p.I379T showed the most irregular deviation pattern in the radius of gyration analysis, followed by the variants p.Y403N and p.R398Q (Fig. 3C). However, the variants p.G250A and p.A291V and the native protein maintained stable compactness throughout the simulation compared to the other proteins. The number of Hbonds was analysed for the variants and native proteins to understand the alterations to the hydrogen bonds among the different proteins. The overall number of Hbonds was found to be between ~265 and ~340 in the native and variant proteins. The variant p.Y403N showed the minimal number of Hbonds until 15 ns. In the last 15 ns of the dynamics run, the variants p.G250A, p.I379T, and p.R398Q showed decreases in number of the Hbonds (Fig. 3D).

## Discussion

In this study, we investigated eight Egyptian patients with IVA that originated from eight unrelated consanguineous families. Three patients were diagnosed during neonatal screening, based on family histories of similar deceased siblings (patients #1, 3, and 8), and five were diagnosed based on the clinical presentation. All patients had abnormal elevations in C5-carnitine in the blood and characteristic organic acid profiles of IVA in the urine. The C5-carnitine values were significantly high in all patients, ranging from a low of 2.45  $\mu\text{mol/l}$  in patient #7 to a high of 17.4  $\mu\text{mol/l}$  in patient #4 (normal C5-carnitine value: 0–0.52  $\mu\text{mol/l}$ ). Isovaleryl glycine was significantly elevated in all patients, with secondary lactic aciduria and ketonuria in patient #2 (Table 1).

Two different clinical phenotypes were observed among our patients: the acute neonatal and chronic intermittent. Five patients manifested the disease with an acute neonatal form (P #1, 3, 4, 7, and 8) that led to multiple neonatal deaths in three families (1, 3, and 8). Three patients (P #2, 5, and 6) showed a milder chronic intermittent presentation; the diagnosis was made at an older age that varied from 13 to 72 months, with little need for dietary restriction and fewer hospital admissions. The prognosis in the intermittent group was more favourable with no permanent neurological sequelae in any of the patients.

## Genotype–phenotype correlation in the eight patients with IVA

We identified nine variants in the eight patients, including four novel variants of which three were missense and one was a frameshift. To date, there are 67 different variants in the IVD gene that are listed in the HGMD; ~73% are missense/nonsense and ~21% are splicing variants. The genotype-phenotype correlation for patients with IVA harboring these mutations is still enigmatic (8,20). The *in silico* prediction tools with the aid of a molecular dynamics analysis have facilitated variant assessments in genetic diseases and provided a potential method to

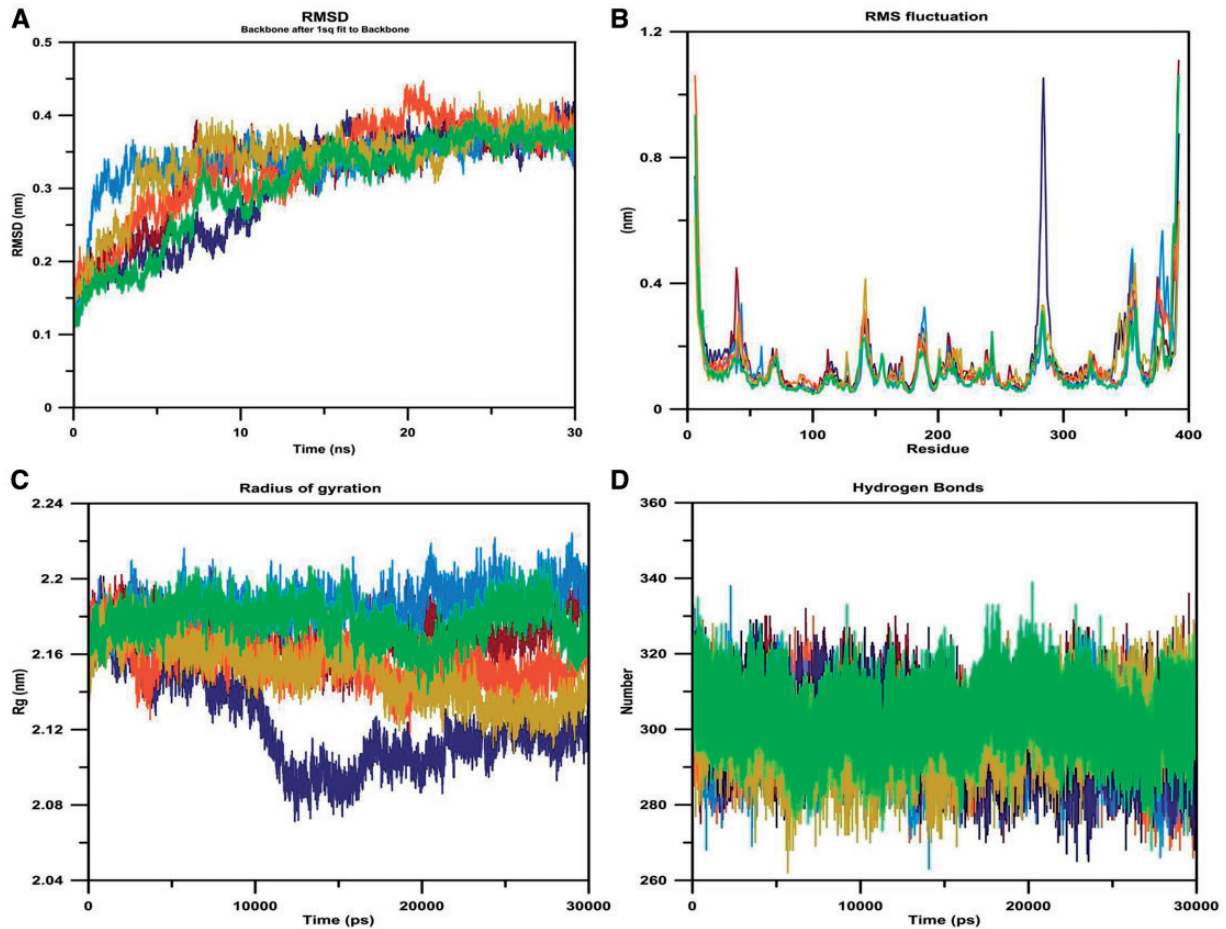


**Figure 3.** Molecular dynamics simulation analysis as a function of the time of IVD native and variants. Color scheme: Native - Green, p.G250A- Sky Blue, p.A291V- maroon, p.I379T- Dark Blue, p.R398Q- Orange, p.Y403N- Brown. (A) Root mean square deviation. (B) Root mean square fluctuation. (C) Radius of gyration. (D) Intramolecular hydrogen bonds.

guide variant classifications and assessments (21–28). In this study, we investigated the potential genotype-phenotype correlations in eight patients by correlating the clinical and biochemical findings from our patients using a different computational prediction analysis, mainly for the five missense variants (p.G250A, p.A291V, p.I379T, p.R398Q, p.Y403N). We used 12 different computational prediction tools to predict the effect of missense variants on protein function. Nine tools were used to predict the pathogenicity of these variants, and three were used to predict the stability of the five protein mutants (Table 3). To strengthen our computational prediction power, we also investigated the protein modeling, macromolecule dynamics, and physiochemical properties of the five mutant proteins. The use of the multiple computational prediction tools can increase the reliability of the predictions of variant classifications (11,24,26,27–30). The successful use of different combinations of computational tools has been previously demonstrated for predicting the potential impact of missense variants on different proteins (25–28,30).

In patient #1, the missense variant p.R398Q that was seen in a homozygous form was predicted to be highly pathogenic and destabilizing by ten out of 12 *in silico* tools (Table 3). The replacement of arginine (R) by glutamine (Q) resulted in several physiochemical changes such as hydrophobic to hydrophilic, a positive to neutral charge and an R' group change from methylene to

amide (Table 4). Furthermore, we also observed higher RMSD values with low compactness (RoG) and a decrease in the number of Hbonds (Fig. 3A, C and D). These alterations could have highly contributed to the higher pathogenicity and destabilizing effect of the variant p.R398Q. The structural visualization by PyMOL showed that the p.R398Q was located in the helical region of the protein (Fig. 4). The p.R398Q variant was previously reported without any further description related to the clinical phenotype and any other clinical parameters (18). Interestingly, the natural history of the patient was consistent with a severe phenotype where two of the patient's untreated brothers had died at the ages of 10 and 11 days (Fig. 2A). In addition, an affected sister, who was diagnosed by newborn screening, died at the age of 3.5 years during a metabolic crisis after a deviation from the strict dietary regimen. Nevertheless, the enrolled patient is doing well on the dietary regimen, and he has developed no neurological sequelae up to the age of three years. Although our data are not conclusive on the potential genotype-phenotype of this variant, the family history, the biochemical and organic acid profiles (Table 1), and the computational prediction results (Figs 2A, 3, 4, and Table 3) suggest a possible genotype-phenotype correlation.

In patients #2 and #8, the p.Y403N was identified as a novel variant in a homozygous form. Patient #2 had an intermediate chronic disease with recurrent cyclic vomiting that started at the age of 2 months and progressed to coma at the age of

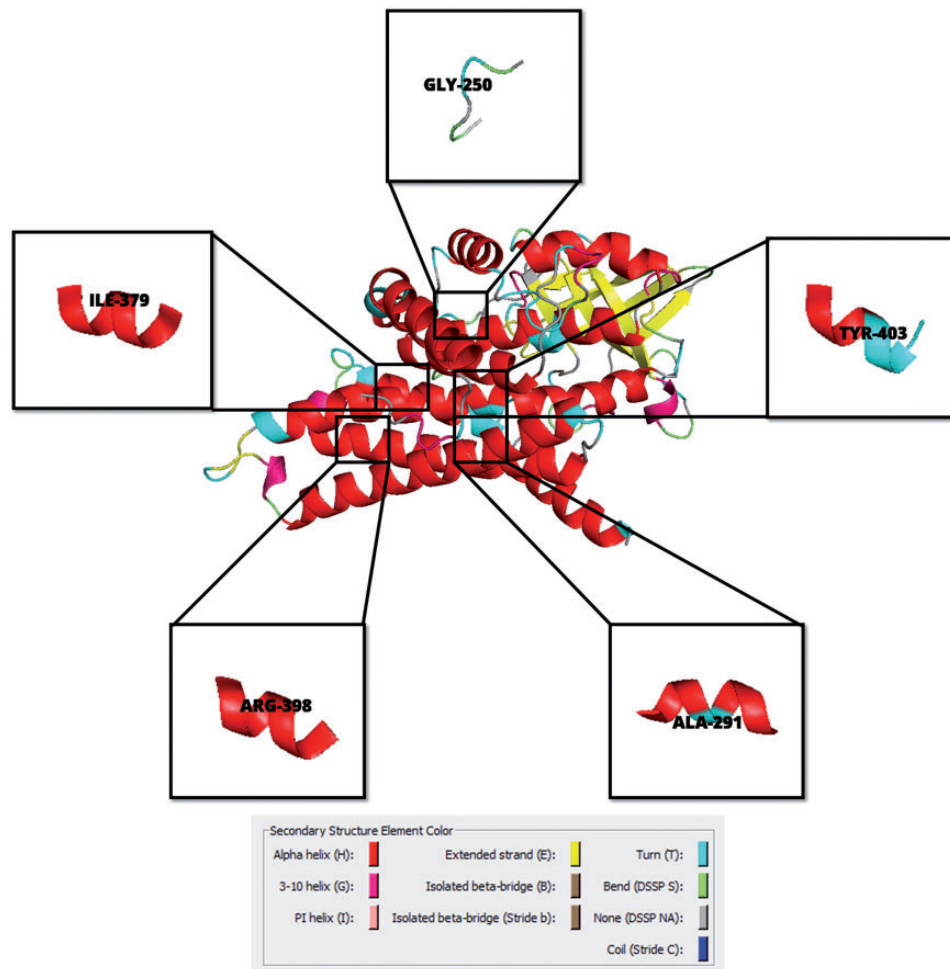


**Figure 4.** The secondary structure visualization of the five variants (p.G250A, p.A291V, p.I379T, p.R398Q, and p.Y403N) was performed using the DSSP plugin of PyMOL. The crystal structure of IVD with PDB ID: 1IVH is represented as a cartoon with the zoomed image illustrating the secondary structural elements of the variants.

1.3 years. Patient #8 was diagnosed during newborn screening due to the previous deaths of two undiagnosed brothers during the neonatal period, with a history suggestive of an inborn error of metabolism. Although the severe presentation was more delayed in patient #2 than in patient #8, the disease was considered as life threatening and required intensive care management of the progressive encephalopathy that led to a coma, which was consistent with the computational prediction of the p.Y403N as pathogenic and destabilizing by seven *in silico* tools (Table 3). The replacement of Tyrosine (Y) by Asparagine (N) resulted in several physicochemical changes, such as side chain flexibility: limited to low, hydrophobic to hydrophilic and an R' group change from hydroxyl to amide (Table 4). The variant p.Y403N is located in the turn region adjacent to the alpha helix where hydrogen bond formations are more favourable (Fig. 4). The absence of this variant in 200 normal chromosomes, the clinically severe phenotypes in the two patients, the abnormal biochemical and organic acid profiles (Table 1), and the computational prediction (Figs 3 and 4 and Table 3) suggest a potential genotype–phenotype correlation for this variant.

In patient #3, c.ins386T was identified as a novel insertion that was absent in 200 normal chromosomes, leading to a frameshift change, p.Y129fs. This variant was found together with two polymorphisms in patient #3 (Table 2); all were in homozygous form. This variant was predicted to be disease-

causing by Mutation Taster and damaging by SIFT. Patient #3 was admitted to the NICU since birth for investigation due to the neonatal deaths of two of her siblings due to IVA. Before the newborn screening results were reported, the patient developed poor suckling, lethargy, convulsions, and hyperammonaemia. She had a significant increase in the C5-carnitine value (10.8  $\mu\text{mol/l}$ ) as well as elevated isovalerate metabolites with secondary lactic aciduria and ketonuria (Table 1). The absence of this variant in 200 normal chromosomes, the early and severe clinical presentation, the biochemical profile for this patient, and the *in silico* predictions by SIFT and Mutation Taster are consistent with the expected consequence of a frameshift variant and may highlight a meaningful genotype–phenotype correlation.

In patient #4, the novel variant p.A291V was identified in a homozygous form. He was admitted to the NICU and presented with poor suckling, lethargy, dehydration, and suspected sepsis followed by hyperammonaemia and thrombocytopenia. The LC-MS/MS revealed marked an elevation of C5-carnitine (Table 1). He received specific treatment for IVA at the age of one month, developed mild hypertension and showed delays in developmental milestones, which were probably due to the delay in diagnosis and initiation of treatment. This variant was predicted to be pathogenic and destabilizing by eight *in silico* tools (Table 3). The replacement of alanine (A) with valine (V) resulted in several physicochemical changes such as side chain flexibility:

limited to low, hydrophobic to hydrophilic and an R' group change from hydroxyl to amide (Table 4). The variant p.A291V is located in the turn region adjacent to the alpha helix where hydrogen bond formations are more favourable (Fig. 4). The severe neonatal clinical presentation, biochemical profiles (Table 1), *in silico* and structural modelling of the mutant enzyme (Tables 3 and 4, Figs 3 and 4), and the absence of this variant in 100 normal individuals are consistent with a potential relationship between the genotype and phenotype for this variant.

In patient #5, the novel variant p.G250A was identified in a homozygous form and predicted to be pathogenic by six *in silico* prediction tools. It was found to be located in the coil region (Fig. 4) where the number of intermolecular hydrogen bonds may be minimal, and this variant may also have minimal effects on the hydrogen bonds (Fig. 3D). These findings were consistent with the milder intermittent vomiting that started at the age of one year in this patient, with no severe neurological manifestations to the extent that he was not suspected of having a metabolic disorder until the age of 5 years, and with the good response to the vegetarian diet regimen without the IVA special formula. The mild elevations in the C5-carnitine values and the mild clinical presentation might suggest a predictable genotype-phenotype correlation of a milder phenotype for this variant.

In patient #6, the splicing variant c.465 + 2T > C was found in intron 4 in a homozygous form (Table 2 and Fig. 1). Human Splicing Finder (13) predicted that the change in the wild-type donor site could most likely affect the splicing. This patient was the second order of birth of a first-cousin consanguineous marriage. He presented with frequent attacks of cyclic vomiting that started at the age of 6 months, with the chronic intermittent phenotype, which led to a delay in the diagnosis until he was referred for a metabolic study at the age of 6 years. However, the C5-carnitine (9.06  $\mu\text{mol/l}$ ) and isovaleryl glycine values were abnormally high. This variant was previously reported ([https://www.ncbi.nlm.nih.gov/projects/SNP/snp\\_ref.cgi?rs=398123683](https://www.ncbi.nlm.nih.gov/projects/SNP/snp_ref.cgi?rs=398123683)), with an allele frequency of minor/major 0.00002471/0.99997526 in 121,412 chromosomes of an aggregated population, and as pathogenic in ClinVar (<https://www.ncbi.nlm.nih.gov/clinvar/variation/94055/>). It was found to alter the stability of the mRNA of the IVD gene and cause abnormal splicing and was suggested to cause a severe clinical phenotype (19). However, the patient had a mild course of the disease with no intellectual or motor sequelae despite receiving no specific treatment until the age of six years. In addition, he showed a marked improvement after following a vegetarian diet regimen. Although this splicing variant is expected to be responsible for a severe phenotype, our clinical data do not support this scale of severity, and our data are inconclusive in predicting a potential genotype-phenotype correlation.

In patient #7, the variant p.I379T was found in a homozygous form. It was predicted to be highly pathogenic and destabilizing by ten out of 12 *in silico* tools (Table 3). These results might be due to the shift in physicochemical properties of the native (isoleucine) and variant (threonine) amino acids such as hydrophobic to hydrophilic, non-polar to polar, and moderate side chain flexibility to low side chain flexibility (Table 4). Similar changes were observed in the variant p.I379T along with the R' group shift from methylene to hydroxyl (Table 4). The p.I379T exhibited a higher deviation (RMSD) with low compactness (RoG) and a decrease in Hbonds (Fig. 3A, C and D). This variant is located in the helical region of the protein (Fig. 4). The absence of this variant in 200 normal chromosomes and the severe neonatal clinical presentation of this patient was consistent with the

*in silico* analysis. However, the patient showed an adequate response to the strict diet and medical treatment that were started one day after her admission, which enabled her to regain consciousness without further crises or complications. Despite the mild elevation of the C5 value (Table 1), the data presented here might indicate a potential relationship between the genotype and phenotype for patient #7.

Although the variants p.I379T (patient # 7; C5 = 2.45  $\mu\text{Mol/l}$ ) and p.R398Q (patient #1; C5 = 6.15  $\mu\text{Mol/l}$ ) were found to be more deleterious and destabilizing compared to the p.A291V variant (patient #4; C5 = 17.4) and p.Y403N (patient #2; C5 = 16  $\mu\text{Mol/l}$ ) and patient #8; C5 = 6.8  $\mu\text{Mol/l}$ ) (Table 3), the four variants were also predicted to be severe by the macromolecular simulation analysis (Figs 3 and 4), which was consistent with the clinical and biochemical profiles of the five patients. It seems that the *in silico* predictions do not correlate well with the biochemical variations of the C5 values for the four variants. This may be due to the inherent limitations of the computational prediction tools or because the biochemical phenotypes of the patients do not necessarily translate to the scale of disease severity for the IVA patients, or it might be that there is a range of C5 concentrations where there no noticeable variability in the disease severity, given the variations in the concentration of the other organic metabolites. The p.G250A variant was computationally predicted as mild, which was consistent with the clinical data of the patients harbouring this variant. It is known, however, that the genotype-phenotype among IVA patients is still questionable. Therefore, to reach a meaningful genotype-phenotype correlation, a large cohort of IVA patients should be investigated. To have a conclusive correlation, these patients should harbour these variants in homozygous form or in compound heterozygous form with another variant that is known to affect protein function. Although the computational analysis on its own is limited in its provision of a conclusive decision about the pathogenicity of a certain variant, it is expected to shed light on the effect of the genetic variation on the function of the protein. In this study, we were able to demonstrate the possible use of correlating the pathogenicity of genetic variants with the clinical phenotype of our patients' cohort. Computational predictions are pragmatic tools for physicians and Variant Scientists to predict the potential pathogenicity of variants, especially variants with no patient data. These predictions are expected to become a powerful tool for future predictions of the disease course in patients detected through newborn screening and their siblings or relatives before the development of the neurological sequelae of the disease.

## Acknowledgement

Hatem Zayed was supported by the Qatar University grant QUU-CAS-DHS-14/15-3.

*Conflict of Interest statement.* None declared.

## Funding

Qatar university grant for HZ SAA and GGM, (QUST-CHS-SPR-2017-17).

## References

1. Vockley, J. and Ensenauer, R. (2006) Isovaleric acidemia: new aspects of genetic and phenotypic heterogeneity. *Am. J. Med. Genet.*, **142c**, 95–103.

2. Matsubara, Y., Ito, M., Glassberg, R., Satyabhama, S., Ikeda, Y. and Tanaka, K. (1990) Nucleotide sequence of messenger RNA encoding human isovaleryl-coenzyme A dehydrogenase and its expression in isovaleric acidemia fibroblasts. *J. Clin. Invest.*, **85**, 1058–1064.
3. Ozgul, R.K., Karaca, M., Kilic, M., Kucuk, O., Yucel-Yilmaz, D., Unal, O., Hismi, B., Aliefendioglu, D., Sivri, S., Tokatli, A. et al. (2014) Phenotypic and genotypic spectrum of Turkish patients with isovaleric acidemia. *Eur. J. Med. Genet.*, **57**, 596–601.
4. Ensenauer, R., Vockley, J., Willard, J.M., Huey, J.C., Sass, J.O., Edland, S.D., Burton, B.K., Berry, S.A., Santer, R., Grunert, S. et al. (2004) A common mutation is associated with a mild, potentially asymptomatic phenotype in patients with isovaleric acidemia diagnosed by newborn screening. *Am. J. Hum. Genet.*, **75**, 1136–1142.
5. Tanaka, K., Budd, M.A., Efron, M.L. and Isselbacher, K.J. (1966) Isovaleric acidemia: a new genetic defect of leucine metabolism. *Proc. Natl Acad. Sci. USA*, **56**, 236–242.
6. Erdem, E., Cayonu, N., Uysalol, E. and Yildirmak, Z.Y. (2010) Chronic intermittent form of isovaleric acidemia mimicking diabetic ketoacidosis. *J. Pediatr. Endocrinol. Metabol.*, **23**, 503–505.
7. Vatanavicharn, N., Liammongkolkul, S., Sakamoto, O., Sathienkijkanchai, A. and Wasant, P. (2011) Phenotypic and mutation spectrums of Thai patients with isovaleric acidemia. *Pediatr. Int.*, **53**, 990–994.
8. Dercksen, M., Duran, M., Ijlst, L., Mienie, L.J., Reinecke, C.J., Ruiten, J.P., Waterham, H.R. and Wanders, R.J. (2012) Clinical variability of isovaleric acidemia in a genetically homogeneous population. *J. Inher. Metab. Dis.*, **35**, 1021–1029.
9. Lin, W.D., Wang, C.H., Lee, C.C., Lai, C.C., Tsai, Y. and Tsai, F.J. (2007) Genetic mutation profile of isovaleric acidemia patients in Taiwan. *Mol. Genet. Metabol.*, **90**, 134–139.
10. Lee, Y.W., Lee, D.H., Vockley, J., Kim, N.D., Lee, Y.K. and Ki, C.S. (2007) Different spectrum of mutations of isovaleryl-CoA dehydrogenase (IVD) gene in Korean patients with isovaleric acidemia. *Mol. Genet. Metabol.*, **92**, 71–77.
11. Bendl, J., Stourac, J., Salanda, O., Pavelka, A., Wieben, E.D., Zundulka, J., Brezovsky, J. and Damborsky, J. (2014) PredictSNP: robust and accurate consensus classifier for prediction of disease-related mutations. *PLoS Comput. Biol.*, **10**, e1003440.
12. Chen, C.W., Lin, J. and Chu, Y.W. (2013) iStable: off-the-shelf predictor integration for predicting protein stability changes. *BMC Bioinformatics*, **14 Suppl 2**, S5.
13. Desmet, F.O., Hamroun, D., Lalande, M., Collod-Beroud, G., Claustres, M. and Beroud, C. (2009) Human Splicing Finder: an online bioinformatics tool to predict splicing signals. *Nucleic Acids Res.*, **37**, e67.
14. Dobson, R.J., Munroe, P.B., Caulfield, M.J. and Saqi, M.A. (2006) Predicting deleterious nsSNPs: an analysis of sequence and structural attributes. *BMC Bioinformatics*, **7**, 217.
15. George Priya Doss, C., Nagasundaram, N., Chakraborty, C., Chen, L. and Zhu, H. (2013) Extrapolating the effect of deleterious nsSNPs in the binding adaptability of flavopiridol with CDK7 protein: a molecular dynamics approach. *Hum. Genomics*, **7**, 10.
16. Guex, N. and Peitsch, M.C. (1997) SWISS-MODEL and the Swiss-PdbViewer: an environment for comparative protein modeling. *Electrophoresis*, **18**, 2714–2723.
17. Pronk, S., Pall, S., Schulz, R., Larsson, P., Bjelkmar, P., Apostolov, R., Shirts, M.R., Smith, J.C., Kasson, P.M., van der Spoel, D. et al. (2013) GROMACS 4.5: a high-throughput and highly parallel open source molecular simulation toolkit. *Bioinformatics (Oxford, England)*, **29**, 845–854.
18. Al-Shamsi, A., Hertecant, J.L., Al-Hamad, S., Souid, A.K. and Al-Jasmi, F. (2014) Mutation spectrum and birth prevalence of inborn errors of metabolism among Emiratis: A study from Tawam Hospital Metabolic Center, United Arab Emirates. *Sultan Qaboos Univ. Med. J.*, **14**, e42–e49.
19. Vockley, J., Rogan, P.K., Anderson, B.D., Willard, J., Seelan, R.S., Smith, D.I. and Liu, W. (2000) Exon skipping in IVD RNA processing in isovaleric acidemia caused by point mutations in the coding region of the IVD gene. *Am. J. Hum. Genet.*, **66**, 356–367.
20. Hertecant, J.L., Ben-Rebeh, I., Marah, M.A., Abbas, T., Ayadi, L., Ben Salem, S., Al-Jasmi, F.A., Al-Gazali, L., Al-Yahyaee, S.A. and Ali, B.R. (2012) Clinical and molecular analysis of isovaleric acidemia patients in the United Arab Emirates reveals remarkable phenotypes and four novel mutations in the IVD gene. *Eur. J. Med. Genet.*, **55**, 671–676.
21. Zhang, Z., Miteva, M.A., Wang, L. and Alexov, E. (2012) Analyzing effects of naturally occurring missense mutations. *Comput. Math. Methods Med.*, **2012**, 805827.
22. Alvares, R.D., Tulumello, D.V., Macdonald, P.M., Deber, C.M. and Prosser, R.S. (2013) Effects of a polar amino acid substitution on helix formation and aggregate size along the detergent-induced peptide folding pathway. *Biochim. Biophys. Acta*, **1828**, 373–381.
23. George Priya Doss, C., Chakraborty, C., Narayan, V. and Thirumal Kumar, D. (2014) Computational approaches and resources in single amino acid substitutions analysis toward clinical research. *Adv. Protein Chem. Struct. Biol.*, **94**, 365–423.
24. Ali, S.K., Sneha, P., Priyadarshini Christy, J., Zayed, H. and George Priya Doss, C. (2016) Molecular dynamics-based analyses of the structural instability and secondary structure of the fibrinogen gamma chain protein with the D356V mutation. *J. Biomol. Struct. Dyn.*, in press., 1–11.
25. Doss, C.G., Alasmar, D.R., Bux, R.I., Sneha, P., Bakhsh, F.D., Al-Azwani, I., Bekay, R.E. and Zayed, H. (2016) Genetic epidemiology of glucose-6-dehydrogenase deficiency in the Arab world. *Sci. Rep.*, **6**, 37284.
26. Zaki, O.K., Krishnamoorthy, N., El Abd, H.S., Harche, S.A., Mattar, R.A., Al Disi, R.S., Nofal, M.Y., El Bekay, R., Ahmed, K.A., George Priya Doss, C. et al. (2017) Two patients with Canavan disease and structural modeling of a novel mutation. *Metab. Brain Dis.*, **32**, 171–177.
27. Mosaeilhy, A., Mohamed, M.M., C, G.P., El Abd, H.S., Gamal, R., Zaki, O.K. and Zayed, H. (2017) Genotype-phenotype correlation in 18 Egyptian patients with glutaric acidemia type I. *Metab. Brain Dis.*, in press.
28. P, S., D, K.T., Tanwar, H., R, S., C, G.P. and Zayed, H. (2017) Structural analysis of G1691S variant in the human filamin B gene responsible for Larsen syndrome: a comparative computational approach. *J. Cell. Biochem.*, **118**, 1900–1910.
29. Capriotti, E., Altman, R.B. and Bromberg, Y. (2013) Collective judgment predicts disease-associated single nucleotide variants. *BMC Genomics*, **14 Suppl 3**, S2.
30. Sneha, P., Thirumal Kumar, D., George Priya Doss, C. and Siva, R. (2017) Determining the role of missense mutations in the POU domain of HNF1A that reduce the DNA-binding affinity: A computational approach. *PLoS One*, **12**, e0174953.